

Color Calibration Optimization

David C. Craig/Xerox Corporation, Shen-ge Wang/Xerox Corporation

Abstract

Color calibration has as its aim consistent color and is constrained by several factors, including both efficiency and contouring. In this paper, we describe a method of color calibration based on the measurement of halftone “quiet levels” and the subsequent selection of 256 halftone levels for CMYK that provide a linear response in dE from paper. The results of this method are contrasted with a more traditional eight bit gray balanced approach to calibration.

Color Calibration Objectives and Constraints

The primary objective of printer color calibration is to bring the printer back to a fixed color response. This response need not be ideal from a preference perspective since destination profiles can be used to make the printer response match the desired source profile. But it is critical that the color response be stable, since destination profiles are typically static or updated infrequently.

Achieving the objective of consistent color response should not, however, be at the expense of other image quality attributes such as contouring. Some calibration approaches can create contours because they reduce the number of distinct gray levels or create steep responses in the tonal reproduction curve.

Calibration Options

Broadly conceived, printer calibration methods can be divided into those that calibrate CMYK individually and those that calibrate CMYK collectively in the form of overlays. In this paper we compare calibration of individual CMYK to linear aims in dE from paper with calibration of CMY overlays to the neutral axis (with separate calibration of K). The ideal method will, of course, depend on printer technology and the extent to which control of individual CMYK controls overlays.

A second dimension relating to selection of calibration method pertains to *how* the aim is achieved. A common approach is to use an 8-bit LUT to map CMYK contone values to alternative values that achieve the calibration aim, whether that aim is gray balanced overlays or single color (CMYK) tonal response curves. One consequence of this approach is loss of gray levels. An alternative approach selects 256 dot levels from the large number of dot levels made available by “sto-clustic” dot designs. The 256 levels are selected so as to achieve the desired response curve and with this approach no gray levels are lost in the calibration process.

Cluster-based printer model

Most digital printers are essentially binary devices. In other words, they are halftone printers. The most common halftone method is screening, which compares requested continuous tone levels to predetermined threshold levels typically defined over a rectangular cell that is tiled to fill the

image plane. The output of the screening process is a binary pattern of multiple small “dots”, which are regularly spaced as determined by the addressability of the imaging system. Marking processes such as electro-photography and offset printing typically cluster the small dots (or activated pixels) within a cell because the larger clustered mass prints with more consistent size and density than spots printed with individual isolated pixels. The alignment of the clusters via the halftone-cell tiling defines the geometry of the halftone screen. The resulting halftone structure is a two-dimensionally repeated pattern, possessing two fundamental spatial frequencies that are completely determined by the geometry of the halftone screen. For example, Fig. 1 shows a typical halftone pattern created by the screening process using a rectangular shape screen with a constant contone input. There is a half-width screen shift between adjacent rows of tiles, so all clusters, or tiles, are aligned in plus and minus 45 degree directions. More realistically, the actual physical output from a printer with the binary halftone pattern in Fig. 1 may look more or less as shown in Fig. 2 with dot overlapping concerned.

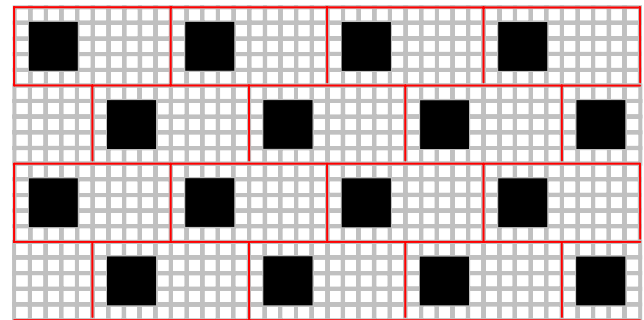


Figure 1. A typical cluster halftone pattern created by a screening halftone process.

The definition of the tile is somewhat arbitrary.¹ In Fig. 2 the tiling effect due to the repeated use of the halftone screen is shown by the red diamond-shape tiles with a different shape from the red rectangular ones in Fig. 1 but the same tile area. In this example, each tile contains exactly the same number of pixels, not only the total number of pixels of each tile, but also the number of printed (black) pixels in each tile. Also, the shape of each cluster structured by grouped black pixels is identical for all tiles. Clearly, for such halftone output with a uniform cluster pattern the average color appearance of each tile should be equal to the overall average color appearance of all tiles, no matter described in which color measure, *e.g.*, spectral reflectance, CIE Lab or density. Therefore, just like a blank paper or a patch completely covered by the solid toner, the color appearance of a single tile can be macroscopically measured directly from a patch printed with a corresponding uniform-

cluster halftone pattern. Of course, we have to assume that the physical area of each cluster, or tile, is much smaller than the area of the color measurement, so the edge effect can be ignored. There is no special printer modeling needed for determining colors for such uniform-cluster halftone patterns.

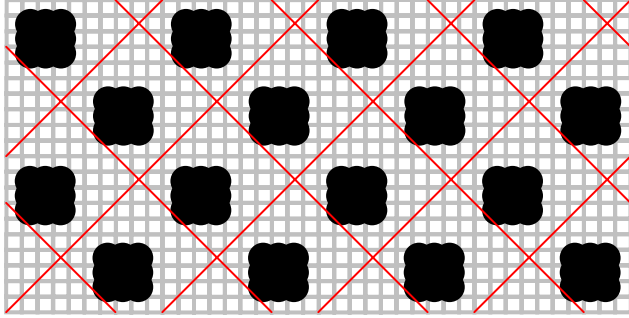


Figure 2. A halftone pattern with uniform-shape clusters. The red lines divide the whole area into two-dimensionally repeated tiles. All tiles contain the same area, the same printed dot cluster.

A single-cell halftone screen uses the entire area of the screen for one cell, or tile, only. Therefore, using a single-cell screen containing N pixels, we can generate $N+1$ different halftone patterns with uniform clusters including the blank paper and the solid output. For such single-cell halftone screens, the halftone outputs can be completely and very accurately determined by direct color measurement. An illustrative raw TRC, which shows the measured delta E (relative to the paper) against the number of printed pixels n ($n = 0, 1, \dots, N$), is directly measured from halftone outputs of a color printer equipped with a single-cell halftone screen with $N = 72$ pixels in its black channel. Altogether there are 73 different halftone patterns with uniform-clusters printed and measured repeatedly. The average result is shown in Fig. 3.

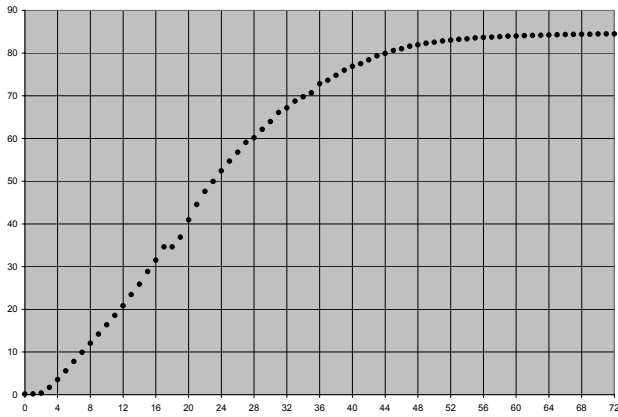


Figure 3. A raw TRC of a single-center halftone screen with $N = 72$ pixels. The TRC is plotted as measured delta E against the number of printed pixels ($n = 0, 1, \dots, 72$).

For most current digital halftone printers, the use of single-cell screens is quite limited because a single cell usually does

not contain a large number of pixels, therefore, it can not provide enough simulated contone levels as desired by most color reproduction tasks. A common approach to overcome this problem is employing halftone screens with multiple (M) centers, such as dual-dot ($M = 2$), quad-dot ($M = 4$) and stochastic (stochastically clustered) screens (M is as large as a few hundreds). Multi-center cluster screens provide much more distinguishable levels for high-quality color output, but also add more difficulties to accurately measure the raw TRCs of the machine. Unlike the single-center screens, it is not practical to get the complete TRC by printing and measuring all $M \times N$ levels. Usually it is solved by some empirical approaches using sampled measurements and purely mathematic functions to determining the TRCs. The drawback of such approaches is that no knowledge of the device physics is concerned; hence, they do not provide the best combination of efficiency and accuracy and, even worse, sometimes yield large errors in derived TRCs which cause contours or other artifacts in final halftone outputs.

Another approach for determining raw TRCs is model based. The well-known Yule-Nielsen modified spectral Neugebauer model² (YNN) is widely used in printing industry. The YNN model, for a halftone patch containing a single colorant can be written as:

$$R^{\frac{1}{\gamma}}(\lambda) = (1-a)R_p^{\frac{1}{\gamma}}(\lambda) + aR_c^{\frac{1}{\gamma}}(\lambda), \quad (1)$$

where $R(\lambda)$ is the average reflectance of the halftone patch at a wavelength λ , a is the fractional area covered by toner, and $R_p(\lambda)$ and $R_c(\lambda)$ are the reflectance of the paper ($a = 0\%$) and solid toner ($a = 100\%$), respectively. The Yule-Nielsen parameter γ accounts the light diffusion in the paper and has a value between 1 and 10 which can be determined by data fitting experimentally and fixed at initial measurement for a certain halftone on a certain hardcopy device. Once the reflectance spectra of the paper and the solid toner are measured, the reflectance spectrum of any halftone pattern can be predicted by the YNN model with an estimated toner coverage a .

The YNN model is quite simple and provides reasonable predictions in many halftone studies. However, the accuracy of its prediction is limited mainly due to the difficulty of estimating the true toner coverage of halftone. The actual outputs from different printers are very complicated. Adjacent printed pixels overlap to each other. Besides, physical halftone outputs have irregular shapes and the size, shape and density vary with time and location. The scattering of the light in the paper substrate adds further complexity, making a detailed microscopic model of the dot overlapping very difficult to construct. Even if with a well defined digital binary description, the true area covered by toner of a halftone pattern is hardly measured and/or calculated accurately.

In this paper, we propose a new method which combines the accuracy obtained from measurement-based approaches and efficiency from model-based ones, especially for raw TRC measurement.

Since a multi-center screen specifies the tiling geometry exactly the same as a corresponding single-cell screen, its

halftone outputs are similar to the ones generated by the single-cell screen, except the printed dot clusters are in general not uniform and vary by its particular design. Again as a common approach in screen design, the difference between clusters at any constant level should be as small as possible to avoid or reduce any possible additional visual noise introduced by utilizing multiple centers in one halftone screen. Consequently, at a constant level, the difference between clusters from this kind of screens is usually only one or few pixels.

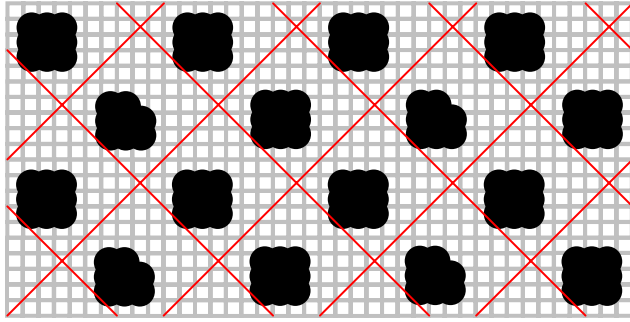


Figure 4. A halftone pattern with two different clusters blended as an output of a multi-center ($M = 4$) halftone screen, or a quad-dot screen.

A typical halftone output from multi-center halftone screen with a constant input level is shown in Fig. 4, where two different printed-dot clusters are blended. It is not difficult to see that all tiles with 9-black-dot clusters in Fig. 4 are identical to the tiles shown in Fig. 2. Therefore, the color of these tiles can be accurately measured using the “calibration patch” described previously for Figs. 1 and 2. Clearly, the color of another kind of tiles in Fig. 4 with 8-dot clusters can be calibrated in a similar matter. Since the ratio between the number of clusters with 8 black pixels and clusters with 9 black pixels is 1/3 in Fig. 4. The overall color of this halftone pattern should be easily determined using a modified YNN model, Eq. (1), with the two spectral reflectance of paper and solid toner replaced by the ones from the two calibration patches.

In a more general form, the cluster-based printer model can be described by the following equation:

$$R^{1/\gamma}(\lambda) = \sum_i^N n_i R_i^{1/\gamma}(\lambda) / \sum_i^N n_i, \quad (2)$$

where $R(\lambda)$ is the average reflectance of a halftone patch at a wavelength λ , N is the total number of different types of tiles, or clusters, involved. The integer n_i is the number of occurrences of the i -th type of tiles and $R_i(\lambda)$ is its spectral reflectance, which can be measured from a printed halftone pattern generated using a corresponding single-center halftone screen. As mentioned previously, for our application of this printer model to measuring raw TRCs by multi-center halftone screens, the total number N in Eq. (2) usually is equal to 2 or a very small number.

Different from the original YNN model, the fractional toner coverage a in Eq. (1) is replaced by the count of tiles, or

$$a_i = n_i / \sum_i^N n_i, \quad (3)$$

in the new printer model and it can be determined directly from the digital binary pattern without any additional modeling, assuming or guessing as previously in the applications of the conventional YNN model. As long as the different part between different tiles, usually just one pixel, is far enough from overlapping the lines defining the tiles, the cluster-based printer model provides very accurate result. Since the defining of tile boundaries is a kind of arbitrary as discussed previously, the above condition is almost always satisfied in our practice.

In our application of the proposed cluster-based printer model, the most interesting cases are blending of two different clusters with very similar size and shape. The two spectral reflectance, $R_1(\lambda)$ and $R_2(\lambda)$, from corresponding uniform-cluster halftone outputs should be also have close values. The average reflectance of the blended halftone pattern described by Eq. (2) can be rewritten as

$$[R_1(\lambda) + (R(\lambda) - R_1(\lambda))]^{1/\gamma} = (n_1 \cdot [R_1(\lambda)]^{1/\gamma} + n_2 \cdot [R_1(\lambda) + (R_2(\lambda) - R_1(\lambda))]^{1/\gamma}) / (n_1 + n_2)$$

or

$$[R_1(\lambda) + (R(\lambda) - R_1(\lambda))]^{1/\gamma} = \frac{n_1}{n_1 + n_2} + \frac{n_2}{n_1 + n_2} [1 + (R_2(\lambda) - R_1(\lambda)) / R_1(\lambda)]^{1/\gamma}. \quad (4)$$

Since $R_2(\lambda) - R_1(\lambda)$, as well as $R(\lambda) - R_1(\lambda)$, is much smaller than $R_1(\lambda)$, taking Taylor series expansion for both sides of Eq. (4) and using only the first non-trivial term of the expansion, we may have approximately

$$1 + \frac{1}{\gamma} \cdot (R(\lambda) - R_1(\lambda)) / R_1(\lambda) = 1 + \frac{1}{\gamma} \cdot \left(\frac{n_2}{n_1 + n_2} \right) (R_2(\lambda) - R_1(\lambda)) / R_1(\lambda).$$

It is easy to see that above equation can be further reduced to a very simple form:

$$R(\lambda) = \frac{n_1}{n_1 + n_2} R_1(\lambda) + \frac{n_2}{n_1 + n_2} R_2(\lambda). \quad (5)$$

In other words, if the two kinds of clusters blended have similar structures and small difference in reflectance, the average output of the blending is simply a linear combination of the two reflectance and the coefficients of the linear combination are given by the counts of each kind of clusters. The value of the Yule-Nielsen parameter γ taken in the printer model, Eq. (2), does not affect the result. Since the approximation, Eq. (5), is true for all wavelengths and CIE XYZ color measures are defined as linear combinations of the full reflectance spectrum, we can derive the average color output of blended clusters as

$$X = \frac{n_1}{n_1 + n_2} X_1 + \frac{n_2}{n_1 + n_2} X_2, \quad (6)$$

where X is the average CIE X (Y , or Z) value of the blended clusters and X_1 and X_2 are the CIE X (Y , or Z) values of the two halftones with uniform-clusters, respectively. Using a similar argument used to derive the approximation Eq. (5), one can easily prove that the statement above, Eq. (6), can be applied to CIE Lab values and the delta E measured in the CIE Lab space, as long as the same assumption about the small difference between the two kinds of clusters for Eq. (5) is held. As a result, the variable X in Eq. (6) can be interpreted as any one of CIE XYZ, CIE $L^*a^*b^*$, density, and deltaE measured in the Lab space. A general formula can be also proved for blending more than two kinds of different clusters as

$$X = \frac{\sum_i^N n_i X_i}{\sum_i^N n_i}, \quad (7)$$

Consider a multi-center halftone screen with M clusters and maximal N pixels in each cluster. Theoretically, altogether there are $M*N+1$ distinguishable halftone patterns created by this screen with constant inputs. If all clusters have the same growth, *i.e.*, the shape of clusters with same number of printed pixels is also same, there are $N+1$ halftones, among the $M*N+1$ ones, with uniform-cluster patterns. Sometimes, they are also referred as quiet levels. These quiet-level patterns are identical to the ones created by a single-center halftone screen with same halftone structure geometry. To derive the complete raw TRC of a multi-center halftone screen, the process might be briefly described by the following steps:

1. generate $N+1$ halftone patches represent the $N+1$ uniform-cluster halftone patterns using a single-center halftone screen;
2. measure the $N+1$ halftone patches and save the color measures (spectral reflectance, XYZ, Lab, density or deltaE) as the $N+1$ quiet levels;
3. all levels different from the quiet levels are halftone patterns by blending two or more different kinds of clusters and their values on the TRC can be calculated by Eq. (6) or (7).

It is easy to see that if all levels of a multi-center cluster screen are limited to blending no more than two quiet levels and the two are different only by one pixel, the complete raw TRC of this screen is a piecewise straight-line curve as the result of connecting color measures of all adjacent quiet levels.

A raw TRC of a stoclustic halftone screen, which has 128 centers and similar halftone geometry to the single-center halftone screen used for Fig. 3 with 72 pixels, is derived by the proposed cluster-based printer model using the measurement result shown in Fig. 3. The complete raw TRC is shown in Fig. 5 below.

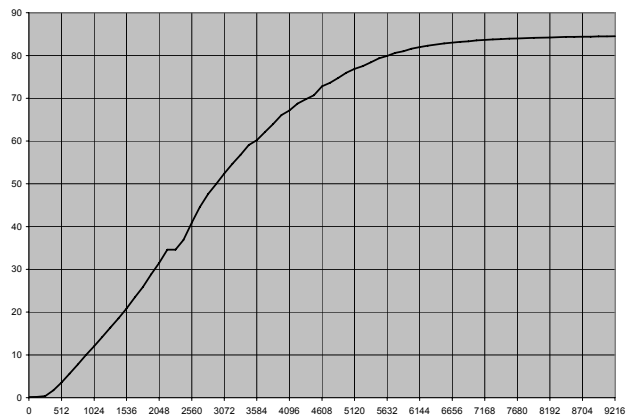


Figure 5. A raw TRC of a multi-center halftone screen with $M = 128$ centers and maximal $N = 72$ pixels in each cluster. The TRC is plotted as measured delta E against the number of printed pixels ($n = 0, 1, \dots, 128*72$).

Results

Two methods of calibration were compared via simulation and print testing. Method 1 uses an 8-bit LUT to gray balance CMY and to separately calibrate K. Method 2 is based on printing all of the “quiet level” dots of a given screen frequency and then finding the 256 dot levels which achieve a linear aim in dE from paper versus contone input (0-255). Both methods were evaluated against various noise conditions. The methods were then compared in terms of color consistency, more specifically, variation from test cell to test cell of 206 input colors.

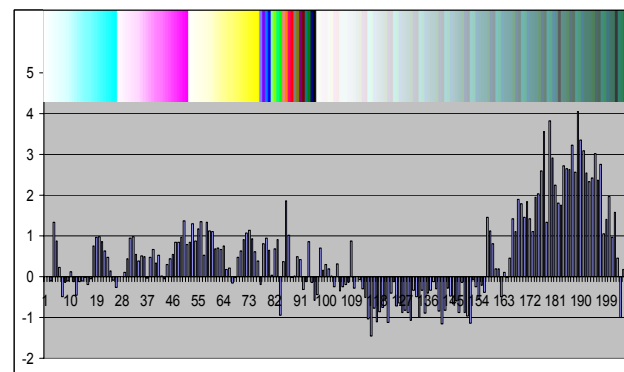


Figure 6. The x axis indicates color patch number and the actual color of the patch is indicted above. Positive values for the y axis indicate how much more maximum dE2000 variation method 1 has than method 2; negative values indicate that method 2 is worse than method 1.

Both simulation (figure 6) and a similar experimental design of experiment showed improvements in overall color consistency with method 2. Overall, in terms of color consistency, calibrating CMYK to linear aims was superior to the method 1 type of gray balanced calibration.

Equally important, method 2 was vastly superior in terms of contouring defects. Because the method results in no loss of gray levels and seeks a linear aim in dE from paper, continuous CMYK sweeps calibrated with this method were remarkable smooth and free of contours. Conversely, with gray balanced calibration based on an 8-bit LUT, the sweeps for some experimental cells showed significant contours. Whereas a linear response in dE gives smooth sweeps, the calibrated CMYK tonal response curves for the gray balanced approach can take a variety of forms, steep and/or shallow, as it attempts to gray balance the engine. Furthermore, because the correction is based on an 8-bit LUT, contouring is further stressed by the fact that gray levels are lost in the calibration process.

References

- [1] S. Wang, Z. Fan and Z. Wen, "Non-orthogonal halftone screens", *Proc. NIP18: International Conference on Digital Printing Technologies*, p578-584 (2002).
- [2] J. A. C. Yule, *Principles of Color Reproduction*, John Wiley & Sons, New York, 1967.

Author Biography

David Craig received his BS in physics from the University of California at Berkeley and an MS in physics and an MS in System Design and Management from the Massachusetts Institute of Technology. Currently, he is an engineering manager responsible for color controls and image based controls.

Shen-Ge Wang received his BS in instrumental mechanics from Changchun Institute of Optics in China and his PhD in optics from the University of Rochester. Currently, he is a principal Scientist working at Xerox Research Center Webster in Webster, NY. His recent work has focused on digital halftoning, printer modeling and digital watermark technologies.